RUNOFF GENERATION CHARACTERISTICS IN TYPICAL EROSION REGIONS ON THE LOESS PLATEAU

Li CHEN [1], Qingquan LIU [2], and Jiachun LI [3]

ABSTRACT

This paper presents a process-based model for runoff generation on slopes. One dimensional kinematic wave theory combined with the revised Green-Ampt infiltration formula is applied in the model. According to the characteristics of soil and rainfall in the Loess Plateau area, six types of storm are defined, and among them three typical erosion zones that have different values of representative parameters are chosen to simulate the runoff generation processes. The primary hydraulic characteristics of the runoff generation, such as unit discharge, runoff depth, flow velocity, shear stress and ratio of runoff generation, are obtained and analyzed. The results demonstrate that the different erosion characteristics are related to different runoff generation zones.

Key Words: Infiltration, Runoff generation, Soil erosion, Loess Plateau

1 INTRODUCTION

The Loess Plateau in the central and western China with an area of 430,000 km^2 is well known for its ancient culture and serious soil and water loss. About 287,000 km^2 of area in this region has an annual erosion rate greater than 1000 t/km^2. The eroded soil totally amounts to more than 2.2×10^9 tons, among which about 1.6×10^9 tons, on average, is delivered into the Yellow River, making the river one of the highest sediment-laden rivers in the world. The serious soil erosion of long time period has led to the fragment geomorphy in this region. Moreover, the recent violent human activities have considerably aggravated the situation and have brought about a series of consequences such as lean soil, land desertification, arable land diminish and reduction of output. The sediment delivered into the Yellow River and carried downstream is responsible for frequent flooding disasters in the middle and lower reaches. Furthermore, the sediment with absorbed toxic elements from pesticide and fertilizer in the cultivated land may cause water pollution, which does harm to the health of human being and animals, by concentration effect. Therefore, it is an urgent, but challenging task to prevent ecological environment deterioration due to soil erosion.

During the recent decades, the soil erosion in the Loess plateau has been extensively investigated. A general qualitative cognition on issues such as erosion type, erosion intensity, erosion geomorphy and their regional distribution has been acquired. At the same time, an in depth understanding of their physical mechanism has been obtained based on numerous laboratory and field experiments. Many empirical and semi-empirical relationships have been established to quantitatively estimate runoff and soil erosion. However, most of the previous researches aiming at a certain specific erosion type or region have covered very limited parameter ranges. As a matter of fact, surface features, topography and soil characteristics of the Loess Plateau along with rainfall conditions are extremely different in various regions. The research results in some specific regions without quantitative comparison and physical exploration is unable to reflect overall roles of various factors in the process of erosion. Therefore, we can hardly identify which one is dominant for such variations.

Present research of soil erosion tends to shift from the empirical approach to the process-based dynamic description. Obviously, the study on the infiltration and runoff has become mature. The famous Green-Ampt model with explicit physical meaning was developed in 1911, then the models of Horton (1940), Philip (1957) et al. in succession. So far the G-A (Green-Ampt) model is still commonly used because of its simplicity and extensive applications. In particular, the improvements by Mein and Larson (1973) and

[1,2,3] Division of Engineering Sciences, Institute of Mechanics, Chinese Academy of Sciences, Beijing 100080, China
E-mail: qqliu@mail.imech.ac.cn

Note: The manuscript of this paper was received in Dec. 2000. The revised version was received in April 2001. Discussion open until Dec. 2002.

Chu (1978) have extended its applicability to the circumstances of steady or unsteady rainfall. Although the Horton model is widely applied in China, the parameters involved do not bear apparent physical meaning. Some researchers have included the coupled soil moisture equation in the model (De Lima, 1992). Nevertheless, it always needs more parameters and CPU time. As for runoff, most researchers prefer to describe overland flows by the so-called kinematic wave theory. Actually, it is a simplified form of the 1-D St. Venant equation. Woolhiser and Ligget (1967) have shown that the result of the kinematic wave theory is close to that of St. Venant equation if the kinematic wave number satisfies the condition of k>10. Actually the kinematic wave number is certainly much greater than 10 on the Loess Plateau as Shen et.al.(1996) reported. Therefore, the kinematic wave approximation turns out a suitable mathematical description of the runoff generation process on the Loess Plateau. Till now there have been some revisions in the kinematic wave model (Ponce et al., 1978, Govindaraju, 1988). If the streamwise variation of water depth is considered by introducing an additional pressure gradient term, it becomes diffusion wave model. Despite the kinematic wave theory is still the principal model in practical applications, the full St. Venant equation system have also been utilized sometimes (Qi and Huang, 1997).

In contrast, the study of the dynamics of erosion process and sediment generation is rather weak. The reason for the situation mainly lies in the fact that the erosion process is so complicated since it includes so many parameters, which are hard to be measured or evaluated. Although the sediment movement dynamics in the river is well developed, it is improper to apply the theory into soil erosion in a straightforward way. The empirical Universal Soil Loss Equation (USLE) established in 1960's and its subsequent revised version (RUSLE) are still extensively used till now. At the same time, the investigation on new process-based models such as WEPP in USA and ANSWERS in Europe are under way. They have advantages in its rich database for all kinds of underlying surfaces and wide applicability. However, this kind of models may not possess a solid physical basis in some degree. Though they were designed based on physical processes, they did not start from basic physical principles in many aspects. Tang and Chen (1997) have presented an elaborate formula for predicting transport capacity of overland flows. This formula seems to be more theoretical and has been applied in some regions, but it can not simulate the dynamic evolution on the slope.

The water erosion process caused by rainfall is a complicated process affected by both water and soil interactively. However, the water flow produces eroding force and plays an active role in the whole process. It is of primary importance to firstly understand runoff generation characteristics. As the first step, the objective of this paper therefore is to examine the runoff generation process in several typical regions on the Loess Plateau by a comprehensive process-based model of rainfall-infiltration-runoff generation. Then their respective characteristics and elucidated physical mechanisms are analyzed, which will certainly be helpful for having an insight into the process of soil erosion.

2 RUNOFF GENERATION MODEL

2.1 Overland Flow Model

When the rainfall intensity exceeds soil infiltration rate, water begins to accumulate on the surface. It is not until the surface ponding capacity being exceeded that water flows down the slope under the action of gravity and form sheet flow. That is just the beginning of runoff generation. Since the depth of overland flow is usually very shallow (of the order of 10^{-3}m) and the boundary on the ground is rather complicated, the description of it is always difficult. At present the one-dimensional kinematic wave model is mostly used. The governing equations are:

$$\frac{\partial h}{\partial t} + \frac{\partial q}{\partial x} = p\cos\theta - i$$
$$q = \frac{1}{n} h^{5/3} S_0^{1/2} \qquad (1)$$

where x is the coordinate along the flow direction(m), t is the time(s), h is the water depth(m), q is the unit discharge(m^2/s), p indicates the rainfall intensity(m/s), i is the infiltration rate(m/s), S_0 is the slope gradient ($S_0 = \sin\theta$), θ is the inclination angle of slope (in degree), and n is the Manning roughness coefficient.

The kinematic wave model is simplified from the 1-D St. Venant equations. The main assumption is that the friction slope of flows equals the slope gradient ($S_f = S_0$) and thus a concise relationship between discharge and water depth is established Woolhiser and Ligget (1967) have shown that this model is suitable for the description of overland flows.

2.2 Soil Infiltration Model

The soil infiltration process is simulated with the revised Green-Ampt model (Mein and Larson, 1973; Chu, 1978). The governing equations may be written as:

$$\begin{aligned} i &= \frac{dI}{dt} = K\left[1 + (\theta_s - \theta_i)S/I\right] \\ I &= Kt + S(\theta_s - \theta_i)\ln\left(1 + \frac{I}{S(\theta_s - \theta_i)}\right) \end{aligned} \tag{2}$$

where I is cumulative infiltration quantity(m), i is the infiltration rate (m/s), K is the saturate conductivity of soil (or infiltration coefficient)(m/s), θ_s is saturate volumetric water content, i.e., the efficient porosity(%), θ_i is the initial volumetric water content (%), and S is the soil suction (m).

The classic Green-Ampt formula is merely applied to ponding water infiltration process on dry soil. Mein and Larson (1973) generalized it to the infiltration process during rainfall. Suppose p is the steady rainfall intensity. Only if p is greater than the infiltration capability, water begins to pond on the ground. In initial stage of rainfall, all the rain infiltrates into soil. According to G-A model, the infiltration rate is decreasing with the cumulative infiltration quantity until up to a certain threshold value. At the moment of i equal to p, ponding occurs. This cumulative infiltration I_p can be derived by the G-A model:

$$I_p = \frac{(\theta_s - \theta_i)S}{p/K - 1} \tag{3}$$

from which the ponding time

$$t_p = I_p / p$$

is yielded. Thus the infiltration rate in the whole process can be expressed as

$$\begin{aligned} i &= p & t \le t_p \\ i &= K\left[1 + (\theta_s - \theta_i)S/I\right] & t > t_p \end{aligned} \tag{4}$$

where I is the cumulative infiltration depth after the ponding time (including I_p). Since ponding does not occur at t=0, the formula should be revised as

$$K\left[t - (t_p - t_s)\right] = I - S(\theta_s - \theta_i)\ln\left[1 + \frac{I}{S(\theta_s - \theta_i)}\right] \tag{5}$$

in which t_s represents the time from t=0 to the time when $I = I_p$ (or i=p). It is assumed that the ponding occurs at t=0, i.e., taking the first stage of rainfall infiltration (before ponding) as ponding infiltration. Therefore we have t_s<t_p. t_s could be looked as a pseudo time. From eq.(2) we have

$$Kt_s = I_p - S(\theta_s - \theta_i)\ln\left[1 + \frac{I_p}{S(\theta_s - \theta_i)}\right] \tag{6}$$

The main idea of revision is to assume the entire process as ponding infiltration from the very beginning. Therefore the whole curve, since ponding starts, should be translated to the left by $t_p - t_s$. By translating this curve back to the right by $t_p - t_s$, we could get the real infiltration process.

However, the steady rainfall is far from the requirements in actual applications. Chu (1978) generalized the GA-ML model again to the unsteady rainfall process. The main procedure is to sort the ground surface status into four types for each time step:

1) no ponding at the beginning, no ponding at the end
2) no ponding at the beginning, ponding at the end
3) ponding at the beginning, ponding at the end
4) ponding at the beginning, no ponding at the end

At the beginning of each time interval, the total rainfall quantity $P(t_{n-1})$, total infiltration quantity $I(t_{n-1})$ and total excess quantity $R(t_{n-1})$ are known. Whether the ponding occurs at the end of the interval can be distinguished by two indices c_u and c_p, where c_u is used for determining whether ponding occurs at the beginning of the interval, while c_p is used for determining whether ponding occurs at the end of the interval:

$$\begin{aligned} c_u &= P(t_n) - R(t_{n-1}) - KSM/(i-K) \qquad & c_u > 0 \ \text{ponding at the end of the interval} \\ & & c_u < 0 \ \text{still no ponding} \\ c_p &= P(t_n) - I(t_n) - R(t_{n-1}) & c_p > 0 \ \text{still ponding at the end of the interval} \\ & & c_p < 0 \ \text{ponding disappears} \end{aligned} \tag{7}$$

where M represents $\theta_s - \theta_i$. Provided that $i < K$, there is no ponding all the time and we needn't use these two indices. With these two indices, we can distinguish the four situations for every time step and calculate t_p and t_s for each situation, respectively. Therefore, the rainfall excess rate of each time step could be obtained.

This comprehensive model is solved with regular numerical method. The main frame of the model is presented in WEPP model (Stone, et al., 1995). However, the specific form of the basic equation has been revised in this paper, such as the effect of the slope gradient on rainfall intensity and infiltration rate is taken into consideration, and the solving manner to the whole system is more direct.

3 MODEL VALIDATION

The laboratory experimental data of Lima(1992) is used to verify the performance of the model. This experiment was proceeded in a flume with length 1 m, width 0.5m and slope S_0=0.1. The rainfall intensity was 0.03741mm/s together with other soil parameters as follows

$$K = 1.67\times10^{-6}\text{m/s},\ \theta_s = 0.506,\ \theta_i = 0.0107,\ S = 0.02\text{m}$$

Fig. 1 is the comparison of calculated results and the experiment of the unit discharge at the outlet. The simulated diagram shows good agreement between them except during the very short initial period. It is especially encouraging to find the consistency between the theory and the experiment when runoff is about to stop. The results indicate that the model presented in this paper could correctly simulate the runoff generation on the slope at least to some degree. Moreover, we have analyzed various factors affecting the major parameters as well as the process of rainfall-infiltration-runoff generation. The following are the principal conclusions:

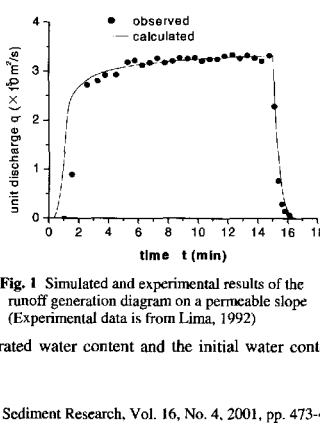

Fig. 1 Simulated and experimental results of the runoff generation diagram on a permeable slope (Experimental data is from Lima, 1992)

1)Each parameter (unit discharge, water depth, flow velocity, shear stress) grows as the rainfall intensity is increasing.

2)Each parameter increases as the infiltration rate is diminishing.

3)Each parameter rises as the slope becomes longer.

4)Each parameter decreases as the volumetric soil water deficiency (the difference between the saturated water content and the initial water content) becomes larger.

5)The increase of slope gradient brings about twofold effects on hydraulic parameters. On the one hand, the rainfall receiving area (the area perpendicular to the rain direction) of the slope becomes smaller as rain is assumed to fall vertically. And so does the received rainfall quantity. On the other hand, the infiltration rate decreases so that the runoff generation increases correspondingly. Under the same runoff generation condition, the sheet depth would become shallow and the flow velocity would increase. To sum up, the discharge rate on the whole decreases as the slope gradient is increasing with the slope length kept constant (It just increases slightly on a very gentle slope). The runoff depth also decreases correspondingly. Hence, the discharge rate curve looks convex, whereas the flow depth curve is concave. The flow velocity and shear stress would increase at first and then began to decrease when the slope gradient reaches their respective critical values. Although the corresponding critical slopes are not equal, both of them are estimated within the range of about 40°~50°(Chen, et al., 2001).

4 SELECTION OF RAINSTORM AND SOIL PARAMETERS

4.1 Partitioning and Selecting of Typical Regions

Generally speaking, the soil erosion intensity is gradually increasing from the south to the north in the Loess Plateau area (Chen et al., 1988; Chen et al, 1996; and Chen, 1996). For convenience, this area could be partitioned into three belts correspondingly, namely clay loess belt, loess belt and sandy loess belt (Liu, 1965). The erosion in these belts possesses their own characteristics. We choose one typical region in each belt and then simulate runoff generation in these typical regions in order to analyze the characteristics of runoff generation under different rain types.

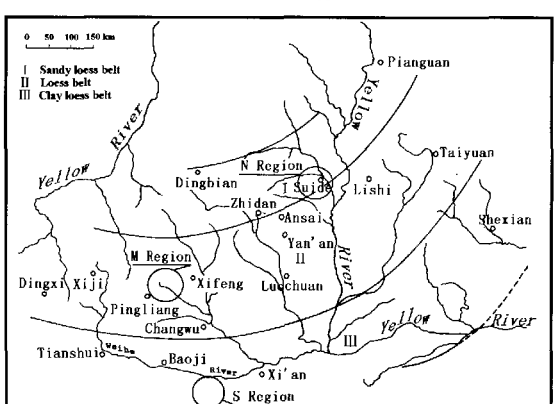

Fig. 2 The skeleton map of the Loess Plateau and the selected typical regions

These three region are: region N is located at the Yellow river valley with extremely intensive erosion in the northeast of Shanxi province just adjacent to Sanxi province. The soil there belongs to sandy loess. Its grain is relatively coarse and the clay content is quite low; region M denotes the area around Gu Yuan -- Ping Liang -- Xi Feng with intermediate intensity of erosion in the central Shanxi, The soil there belongs to loess and its property is between clay and sandy loess; region S is at the Weinan plain with slight erosion intensity. The soil there belongs to clay loess. Its grain is relatively fine and the clay content is high.

The modeled slopes are all assumed flat and barren without any vegetation cover. The calculated slope length is 30m in each case study. We take the average values of the slope distribution provided by Jiang

(1997) as slope gradient. Among them, the values of Sui De are used for N region. Though the erosion is also extremely intensive in the region north of Sui De, the place belongs to the typical region of hybrid wind-water erosion. The effect of wind is prominent. In the long run, the slope inclination of regions N, M, S are selected as 28°, 22.6°, 14.3°, respectively.

4.2 Determination of Rainfall Process

What is unique for the erosion on the Loess Plateau is that it always occurs during rainstorm. The rainfall numbers giving rise to apparent erosion do not exceed 10% of total ones. On average, three rainfalls in each year may cause serious erosion, only occupying about 4% of total rainfall times. As roughly estimated, 80% of total erosion quantity is yielded in 1.3 times of rainfall while 50% of total erosion quantity in 0.6 times of rainfall (Wang & Jiao, 1996). Thus we would rather lay emphasis on the erosion of the Loess Plateau under rainstorm conditions.

Since there are no standard rainfall frequency and rain intensity available according to Wang and Jiao (1996), we chose a uniform rainstorm, three sorts of Type A rainstorm and two sorts of Type B rainstorms and design the rainfall patterns for each case of the two types. Type A rainstorm is assumed as a single-peak rain process of short duration with high peak while Type B rainstorm as multi-peaks rain process of long duration with relatively low peak in which one peak value is equal to 3~5 times of the others. The whole duration of Type A rainstorm is 1 hour and the total rainfall is 60 mm while 6 hours and 120 mm for Type B rainstorm (with two peaks). The peak of type A1 is in the middle of the duration, the peak of type A2 at the beginning and the peak of type A3 at the end. The higher peak of Type B1 is before the lower peak and the Type B2 is just the opposite. These diagrams are shown in Fig. 3.

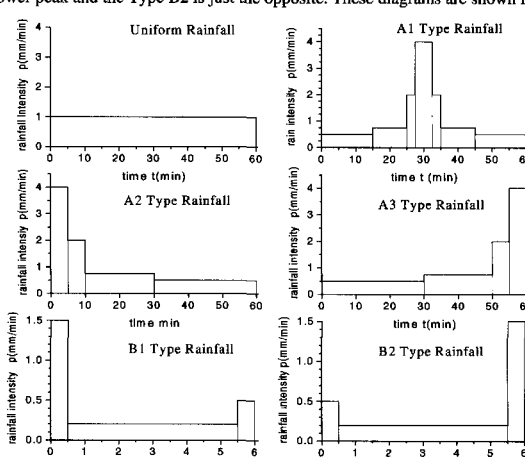

Fig. 3 Rainfall Process for Calculation

4.3 Soil Characteristic Parameters

The basic soil characteristics have great effects on the runoff generation and soil erosion process. Many scholars have carefully investigated the characteristics of soil in the Loess Plateau region. According to the previous research, we have determined the characteristic parameters in the three typical regions in Table 1.

Table 1 Soil characteristic parameters

Parameter	N region	M region	S region
Infiltration coefficient K(mm/min)	0.75	1.08	0.92
Porosity θ_s(%)	57	55	50
Initial moisture weight percentage (%)	14.4~50%	21.0~70%	20.7~70%
Soil suction S(m)	0.06	0.10	0.15
Roughness coefficient n	0.03	0.03	0.03

The following are some remarks in choosing these parameters:

(1) The porosities according to Jiang (1997) are used.

(2) The initial volumetric soil contents are based on the conclusion by Yang (1996) that the natural water content is 50% of the field moisture capacity in sandy loam region and 70%~80% in medium loam and heavy loam regions in general. However, the field moisture capacity is assumed to be the results observed by Yang (1996) through a transfer from moisture weight percentage to volumetric water content in terms of dry soil bulk density.

(3) The measured data of infiltration coefficients by Jiang (1996) are applied, but they are apparently larger than real values so that even extraordinary storm is unable to generate runoff. On the one hand, the experiments were done using two-loop method which is commonly thought to account for the error due to the instrument. On the other hand, the topsoil would crust under the impact of raindrop in actual rainfall process and then finer particles fill in the pore thus rendering the surface soil relatively impermeable to water. According to the comparison of Jiang (1996), the measured infiltration coefficient is about three times as large as the calibrated ones by hydrology method. Thus we first divide the measured value by 3. Secondly, infiltration rate calibrated by hydrology method is not physical parameter, but a kind of average value of the entire process. For steady rainfall it equals the average infiltration rate of the whole process while for unsteady rain it is generally slightly greater than the average infiltration. However, when rainfall intensity is greater than the infiltration coefficient, the infiltration rate is always greater than the saturated conductivity of soil. Therefore, the infiltration rate calibrated with hydrology method is still greater than the actual physical infiltration coefficient. Thus we multiply the measured value by 0.5 in addition as the estimation to the real value. That is to say, we eventually divide the measured value by 6.

(4) The experimental formula of Jiang is adopted to reflect the effect of slope on infiltration rate, i.e., the infiltration coefficient K now becomes $K(1-\sin\theta)$.

(5) There seems no credible soil suction available in the Loess Plateau region. We can only follow the U.S standard given by Chu (1978).

(6) The roughness coefficient is assumed 0.03 by referring to Chen (1994) and Qi (1997).

5 ANALYSIS OF RUNOFF GENERATION CHARACTERISTICS

We have calculated six types of rainfall respectively, that is, three Type A rainstorms, two Type B rainstorms and uniform rainstorm. The results are shown from Fig. 4 to Fig. 9. The diagrams of unit discharge q, water depth h, flow velocity u, shear stress τ varying with time at the slope outlet is given for each rain type. Fig. 4 is the results for uniform rainfall case. Fig. 5~7 are for type A rainstorms while Fig. 8~9 are for type B rainstorm. In each figure, 'nor' means the corresponding curves in region N, 'mid' means those in region M and 'sou' means those in region S. We'll address these problems in the following :

5.1 Runoff Generation Ratio

The runoff generation ratio is defined as the ratio of the runoff volume (or depth) to the rainfall volume (or depth), a physical quantity exhibiting relative strength of runoff generation. The calculated results of the runoff generation ratio in every region and for every rain type are listed in Table 2.

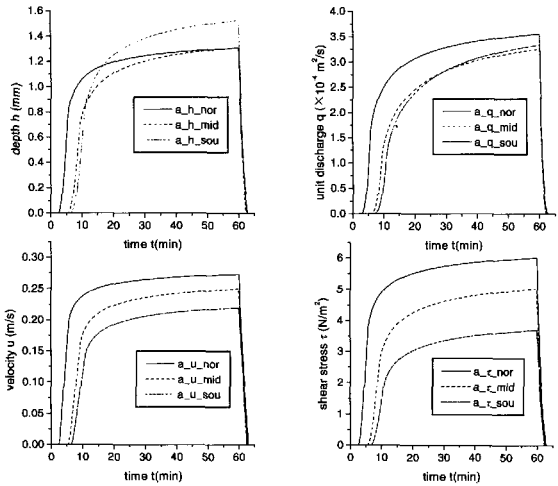

Fig. 4 Runoff generation process of uniform rainfall

Table 2 Runoff generation ratio of every typical region under different rainfall

Rain Type \ Region	N region	M region	S region
Uniform	0.666	0.518	0.485
A1	0.680	0.556	0.529
A2	0.664	0.509	0.474
A3	0.678	0.559	0.537
B1	0.497	0.301	0.281
B2	0.502	0.332	0.322

The runoff generation ratio is mostly above 50% for Type A rainfall, or even near 70% in some area. In contrast, it is around 30% for Type B rainfall or near 50% in some cases. This result is consistent to the conclusion by Wang and Jiao (1996), implying reasonable selection of parameters as well as reliable simulation of the process. We can find from the table that the runoff generation rate is increasing from the south to the north. In the context of runoff generation, we can predict that the erosion force in the north region is stronger than that in south region under the same rainfall condition. Furthermore, the comparison of different rain type shows that the runoff generation ratio of Type A rainstorm is always larger than that of Type B. And the later the peak of rainfall intensity appears, the larger the runoff generation ratio. Thus the rainfall with later peak exhibits more powerful erosion capability than that with earlier peak.

5.2 Runoff Generation Characteristics of Uniform Rainfall

Fig. 4 is the calculated diagram of time evolution for unit discharge q, runoff depth h, flow velocity u and shear stress τ in the three regions under the uniform rainfall. It shows that the moment of runoff

occurrence becomes earlier from the south to the north under the uniform rainfall. It also shows that the duration of 60 minutes rainfall is still far from the steady state of runoff generation process. Every hydraulic parameters rise rapidly in the initial stage of runoff generation. Subsequently, the parameters in region N (the Yellow River valley region in the north) is much larger than those of region M (the middle reach of Jinghe River) and region S (the Wei Nan plain in the south), while the latter two are close to each other. Furthermore, the flow velocity and shear stress grow obviously from the south to the north. Correspondingly, the flow depth of region S is the largest. Very likely, less infiltration and soil suction resulting in large runoff generation account for the foregoing simulated results. Finally, we conclude that the erosion force in the Loess Plateau area is strengthening from the south to the north.

5.3 Runoff Generation Characteristics under Type A Rainfall

The runoff generation results of three Type A rainfalls are shown in Fig.5~7, from which we may find some differences in the characteristics of runoff discharge between the three Type A rainstorms and uniform rainstorm.

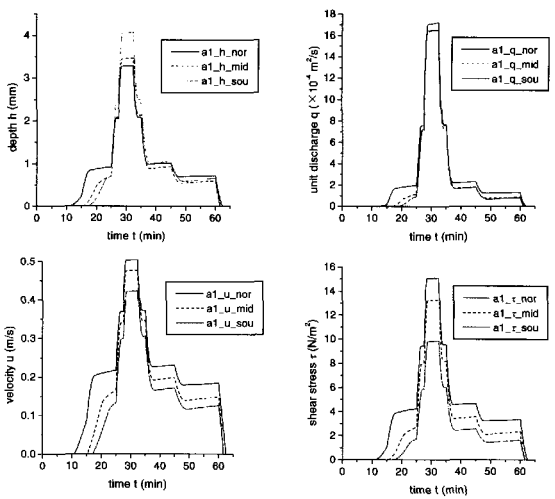

Fig. 5 Runoff generation process of A1 type rainfall

Fig. 6 shows that there are quite small differences between discharge peaks in the three regions under Type A2 rainstorm. The earlier peak value of Type A2 rainstorm leads to the runoff appearance quickly when rainfall starts. During the latter low intensity rainfall, the soil infiltration rate decreases greatly in almost saturated soil so that the runoff may maintain. Although the discharge amounts in three regions are close, the velocity and shear stress seem to be quite different due to different geomorphy.

Fig. 5 and 7 demonstrate the flow discharge peaks in region S are greater than in regions M and N under both Type A1 and Type A3 rainstorms. This phenomenon may attribute to temporal variation of infiltration rate. Although the infiltration coefficient (the ultimate steady infiltration rate) is the lowest in region N, the infiltration rate of wet soil in region S decreases quickly under very high intensity of rainfall, even lower than those in regions M and N. Therefore it leads to more rainfall excess and higher runoff discharge in the south region. The reason for this is quite related to the soil grain size, while the other parameters such as the saturated water conductivity, the water content deficit, the slope gradient, et al.

also have large effect on it. However, the relative magnitude of water depth, flow velocity and shear stress are almost the same as that of uniform rainfall. The results also show that the later the peak value of rainfall, the more difference of runoff generation moments between the three regions. Since the infiltration capacity of region N is the lowest, runoff may occur the earliest under relatively small rainfall. This is responsible for the fact why region N is subjected to longer period of erosion under rainfall with later peak. Also, the maximums of hydraulic parameters are larger for the rainfall with later peak.

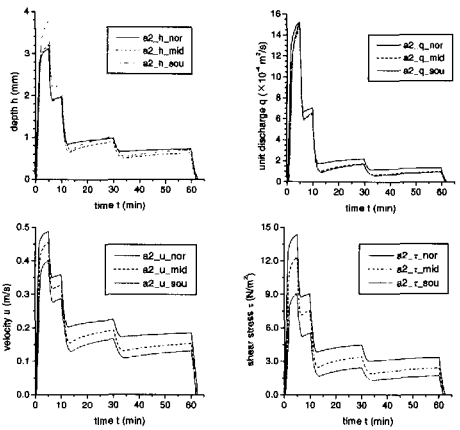

Fig. 6 Runoff generation process of A2 type rainfall

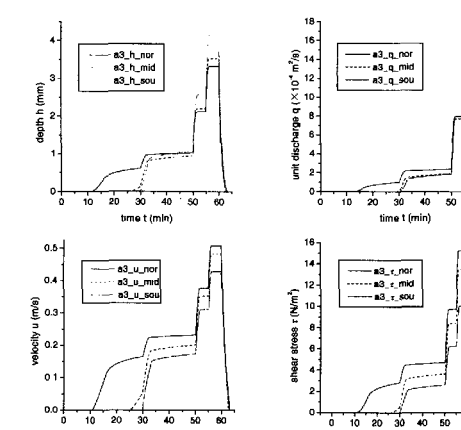

Fig. 7 Runoff generation process of A3 type rainfall

International Journal of Sediment Research, Vol. 16, No. 4, 2001, pp. 473-485

All the figures show that the hydraulic parameters decrease rapidly and then increase moderately when high intensity rainfall turns to low intensity rainfall, and they increase directly when the opposite situation occurs. It is easy to understand that after the previous high intensity runoff flows down the slope the runoff should naturally become of low intensity. When low intensity rainfall changes to high intensity rainfall, the main parameters increase very rapidly. It is because both the infiltration rate decreases and the excess rate increases very rapidly. The conclusion can also be verified by the infiltration formula. It warns us that sudden occurrence of high intensity rainstorm may result in the burst of torrential runoff generation.

In addition, there is a phenomenon in all the three regions: the latter the rainfall peak value, the higher the maximum value of each main parameter. Since the initial period of rainfall makes the infiltration process pass the rapidly decreasing stage, the infiltration rate becomes lower and steadier and the excess rate becomes higher with time for the same intensity of rain. The character infers the latter the rainfall peak value the higher the erosion capability of runoff at the moment of peak value.

5.4 Runoff Generation Characteristics Under Type B Rainstorm

Figs. 8~9 are the calculated results of Type B rainstorms.

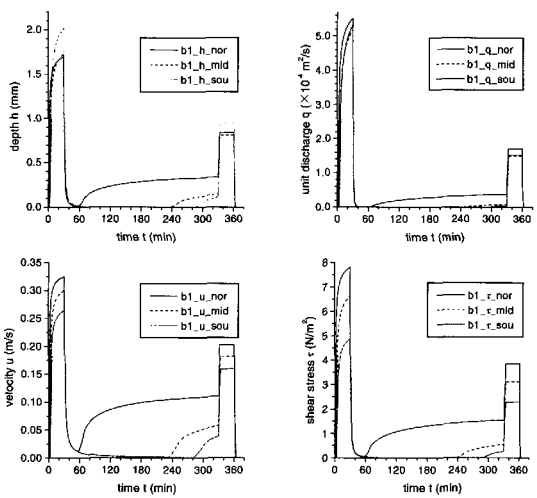

Fig. 8 Runoff generation process of B1 type rainfall

Type B rainfall belongs to of multi-peak and long duration rainfall, generally the maximal peak is 3~5 times of others. The higher peak of Type B1 rainfall is earlier and that of Type B2 rainfall is later. The figures show that the relative magnitude of hydraulic parameters at the moment of high peak is similar to that of the uniform rainfall. Nevertheless, they are the largest at the moment of low peak in region N. The reason is that the soil infiltration is obvious initially so that runoff generation hardly occurs in Regions S and M. All the hydraulic parameters at the moment of high peak for Type B2 rainfall are higher and more steady than those for Type B1 rainfall. It means the rainfall of Type B2 displays higher erosion capability during this period. However, the variation of parameters under two type of rainfall are similar during longer low rainfall intensity period. The runoff amounts are all not very large. It is small in

region M and nearly absent in region S. Only region N shows evident runoff generation. In actual situation, Type B1 rainfall will definitely produce some rills on the lower part of slope and leads to higher erosion rate in latter period due to the existence of rill. As compared with Type B2 rainfall case, the Type B1 rainfall during this period has more erosion capability. However, the erosion during high intensity rainfall of peak value is eventually dominant. Consequently, type B2 rainfall with later higher peak exhibits higher erosion capability.

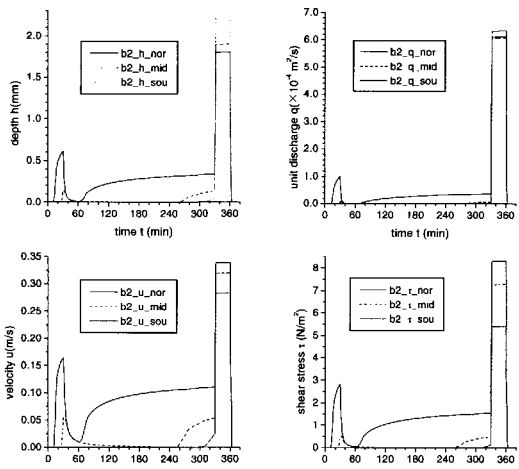

Fig. 9 Runoff generation process of B2 type rainfall

As compared with the Type B rainstorm, the maximums of hydraulic parameters under Type A rainfall are higher, whereas the duration is shorter. It is hard to say which type exhibits higher erosion capability only according to rainfall conditions. The erosion-resistance capability of soil should be considered simultaneously. Generally speaking, type B rainfall with certain intensity and longer duration may erode more soil with low erosion resistance capability than type A rainfall. In contrast, type A rainfall with higher intensity and shorter duration may erode more soil with higher erosion resistance capability than type B rainfall. The specific values of all the parameters should be considered simultaneously.

6 CONCLUDING REMARKS

By simulating the runoff generation process in the Loess Plateau region under different types of rainfall conditions, the runoff generation characteristics in different erosion intensity regions have been carefully studied. The main conclusions are drawn as follow:

1. Under the same rainfall condition, the runoff generation ratio in the Loess Plateau region tends to increase from the south to the north. The hydraulic parameters,, such as unit discharge, flow velocity, and shear stress which are regarded as decisive factors of the erosion quantity, generally coincide with this tendency.

2. The runoff generation ratio of Type A rainstorm with shorter duration and higher intensity is higher than that of Type B rainstorm with longer duration and relatively lower intensity. The peak values of flow

parameter for Type A rainfall are higher than those for type B. The effects of the two types of the rainfall manifest themselves differently in different region.

3. Generally speaking, the later the peak of rainfall is, the higher the peak values of runoff generation parameters and the higher the erosion capability of sheet flows are.

4. The measurement of soil parameters is an indispensable task, which more attention should be paid to in the near future.

5. The present simulation is basically one kind of quantitative investigation under more or less ideal circumstances such as taking average for rainfall and slope and with no regard to vegetation coverage effects etc. They may give rise to the deviation of the typical situations from the actual ones to a certain degree. Due to the limitation of database available, some uncertainty is included in the determination of important parameters such as infiltration and soil suction, which also exerts effects on the calculated results. Despite the foregoing factors, the conclusions we have made are essentially well-grounded and believable.

ACKNOWLEDGMENT

This work is sponsored by the key project of Chinese National Natural Science Foundation (Project No. 19832060) and the foundation of the Chinese National Key Laboratory of Soil Erosion and Dry Land Farming in Loess Plateau

REFERENCES

Chen, G. X.; Xie, S. N.; and Tang, L. Q. 1996, On the erosion and sediment generation model of watershed in Loess Plateau Region. Soil and Water Conservation in Loess Plateau, ed. by Q. M. Meng, Yellow River Hydraulic Press, Zhengzhou. (in Chinese)

Chen L.; Liu, Q. Q.; and Li, J. C. 2001, Study on the runoff generation process on the slope by numerical simulation. Journal of Sediment Research, No. 4, pp. 61-67. (in Chinese)

Chen, Y. Z. 1996, Soil Erosion in Loess Plateau. Soil and Water Conservation in Loess Plateau. ed. by Q. Meng, Yellow River Hydraulic Press, Zhengzhou. (in Chinese)

Chen, Y., Z.; Jing, K.; and Cai, Q. G. 1988, Modern Erosion and Regulation in Loess Plateau, Science Press, Beijing. (in Chinese)

Chu, S. T. 1978, Infiltration during an unsteady rain. Water Resour. Res., Vol. 14, No. 3, pp. 461-466.

De Lima, J. L. M. P. 1992, Model KINNIF for overland flow on pervious surface. Overland Flow, A. J. Parsons and A. D. Abrahams (eds), UCL Press, pp. 69-88.

Govindaraju, R. S. 1988, On the diffusion wave model for overland flow. Water Resour. Res., Vol. 24 No. 5, pp.734-754.

Horton, R. E. 1940, An approach toward a physical interpretation of infiltration-capacity. Soil. Sci. Soc. Am. Proc., Vol. 5, pp. 399-417.

Jiang, D. S. 1997, Soil and Water Loss in Loess Plateau and the Regulation Mode, Hydraulic and Water Power Press of China, Beijing. (in Chinese)

Liu, D. S. 1965, Loess Accumulation in China, Science Press, Beijing. (in Chinese)

Mein, R. G., and Larson, C. L. 1973, Modeling infiltration during a steady rain. Water Resour. Res.,Vol. 9, No.2, pp. 384-394.

Philip, J. R. 1957, The theory of infiltration. Soil. Sci., Vol. 84, pp. 254-264.

Ponce, V. M.; LI, R. M.; and Simons, D. B. 1978, Applicability of Kinematic and diffusion models. J. Hydraul. Div. Amer. Soc. Civil. Eng., Vol. 104, pp. 353-360.

Qi, L. X., and Huang, X. F. 1997, The numerical simulation on runoff generation and soil erosion on slope, ACTA, Mechanica Sinica, Vol. 29, No. 3, pp.343-347. (in Chinese)

Shen, B. 1996, Finite Element Simulation on Surface Hydrology, Press of Xibei Technology University, Xi'an. (in Chinese)

Stone, J. J.; Lane, L. J.; Shirley, E. D.; and Herandez, M. 1995, Hillslope Surface Hydrology. USDA-Water Erosion Prediction Project (WEPP), NSERL Report No. 10, 4.1-4.20.

Tang, L. Q., and Chen, G. X. 1997, The dynamic model of runoff and sediment generation in small watershed, J. Hydrodynamics, Ser. A, Vol. 12, No.2, pp. 164-174. (in Chinese)

Wang, W. H., and Jiao, J. Y. 1996, Rainfall and Erosion Sediment Yield in Loess Plateau and Sediment Transportation in the Yellow River Basin, Science Press, Beijing. (in Chinese)

Woolhiser, D. A., and Ligget, J. A. 1967, Unsteady, one dimensional flow over a plane—The rising diagram. Water Resour. Res., Vol. 3, No.3, pp. 753-771.

Yang, W. Z. 1996, On soil moisture in Loess Plateau. Soil and Water Conservation in Loess Plateau, ed. by Q. M. Meng, Yellow River Hydraulic Press, Zhengzhou. (in Chinese)